Supporting information

Room-Temperature Spin-Coatable Polyoxometalate Composites for High-Contrast, Large-Area Electrochromic Capacitive Films

Shi-Ming Wang*[a,b,c], Kai-Hua Wang[a,b], Lu Zhou[a,b], Tianyang Lu[a,b], Eunkyoung Kim*[c], Zhengbo Han*[b], Jun Liang Lin [a], Lin Liu [b], Guodong Li[d]

a: Light Industry College, Liaoning University, 66 Chongshan Middle Road, Huanggu District, Shenyang 110036, China

b: College of Chemistry, Liaoning University, 66 Chongshan Middle Road, Huanggu District, Shenyang 110036, China

c: Department of Chemical and Biomolecular Engineering, Yonsei University, 50 Yonsei-ro, Seodaemun-gu, Seoul 03722, Korea

d: Shenyang Liaohe Special Glass Factory, 10 A, Zhongyang Road, Offshore Economic Development Zone, Liaozhong District, Shenyang, China

Email: wangsm@lnu.edu.cn (S. M. Wang); ceshzb@lnu.edu.cn (Z. Han); eunkim@yonsei.ac.kr (E. Kim)

1. Experimental section

1.1 Synthesis of P_2W_{18}

The P_2W_{18} was prepared according to the literature [1]and the details are as following: In a 2 L beaker a sample of 250 g (0.76 mol) of $Na_2WO_4 \cdot 2H_2O$ is dissolved in 500 mL of water and 210 mL (3.09 mol) of orthophosphoric acid (85%) is added. The solution is heated at reflux for 4 h. The greenish coloration can be removed by addition of a few drops of bromine or H_2O_2 to the hot solution. (Bromine is very toxic by inhalation and causes severe burns. Work in well-ventilated fume hood and wear gloves. If H_2O_2 is used, the color change will occur in approximately 10 minutes. This choice is safer than bromine, but it comes with the trade-off of a slower reaction rate.) After cooling, l00 g of ammonium chloride is added, and the solution is stirred for 10min. The pale-yellow salt is removed by filtering, then a 25 g quantity of potassium chloride is added to the filtrate to precipitate crude P_2W_{18}, which is collected on a filter and air dried for 2 days. For purification it is dissolved in 200 mL of warm water (ca. 40 ^oC), acidified to pH 2 with HCl, and left to evaporate at room temperature. After several days 123 g of yellow crystals are collected.

1.2 Spin coating of the P_2W_{18} film using different solvent

P_2W_{18} (2 g) was dissolved in 10 mL 1:1 water-ethanol (v:v) mixture **(F1**), dimethyl sulfoxide (DMSO, **F2**) to make a solution for spin coating as reported in the literatures. [2, 3]

1.3 Preparation of HKUST-1 modified FTO substrate

First, a layer of copper octahedral seeds was electrodeposited on the FTO substrate under -0.6 V for 300 s, and then HKUST-1 was attached to the grown copper surface using anodic electrodeposition under 0.8 V for different time in trimesic acid (**BTC**) solution. During that process, copper was oxidized to Cu^{2+} and react with BTC. The HKUST-1 (**H**) layers with different deposition times (60 s, 90 s, 120 s, 150 s) was denoted as H60, H90, H120, and H150, respectively.

1.4 Spin coating of the P_2W_{18}-PVA film on various substrates

FTO, HKUST-1 modified FTO and ITO-PET were employed as the substrate in this

paper. The spin coating procedure is the same for different substrate. The thickness of the films was determined by the concentration of the P_2W_{18} and PVA which was detailed in Table 1 in the manuscript.

1.5 Fabrication of MnO_2 Electrodes with Different Thickness

The MnO_2 film was prepared using the constant potential electrodeposit method according to the literature. [4] The 0.1 M aqueous solution of $Mn(CH_3COO)_2$ and Na_2SO_4 was prepared as an electrolyte for electrodeposition of the MnO_2 film. Under a constant potential of 0.6 V (*vs.* Ag/AgCl), electrodeposition was carried out for 50 s, 100 s, 150 s, 200 s, and 250 s to obtain MnO_2 electrodes with different thicknesses, denoted as M1-5.

2. Characterizations

The characterization of electrochromic performance of the ECDs was carried out using the electrochemical workstation (CHI600D) and UV-vis spectrophotometer (UV-2550). The reference of the UV-vis measurements was the as prepared device. The morphologies of in-situ growth HKUST particles on FTO, P_2W_{18}-PVA and HKUST-P_2W_{18}-PVA films was observed by HITACHI SU8000 scanning electron microscope. The crystal structure of HKUST was characterized by Bruker D8 powder X-ray powder diffractometer (XRD).

Reference

[1] R. Contant, W.G. Klemperer, O. Yaghi, Potassium Octadecatungstodiphosphates(V) and Related Lacunary Compounds, Inorg Synth 1990, pp. 104-111. https://doi.org/10.1002/9780470132586.ch18.

[2] S. Takano, A. Kishimoto, K. Hinokuma, T. Kudo, Electrochromic thin films coated from peroxo-polymolybdotungstate solutions, Solid State Ionics 70-71 (1994) 636-641. https://doi.org/10.1016/0167-2738(94)90385-9.

[3] T. He, Y. Ma, Y. Cao, W. Yang, J. Yao, Preparation and electrochromism of alkylammonium molybdate thin films, J. Non-Cryst. Solids 315(1) (2003) 7-12. https://doi.org/10.1016/S0022-3093(02)01575-2.

[4] S.-M. Wang, Y.-H. Jin, T. Wang, K.-H. Wang, L. Liu, Polyoxometalate-MnO2 film structure with bifunctional electrochromic and energy storage properties, J Materiomics 9(2) (2023) 269-278. https://doi.org/10.1016/j.jmat.2022.10.007.

3. Supporting Figures

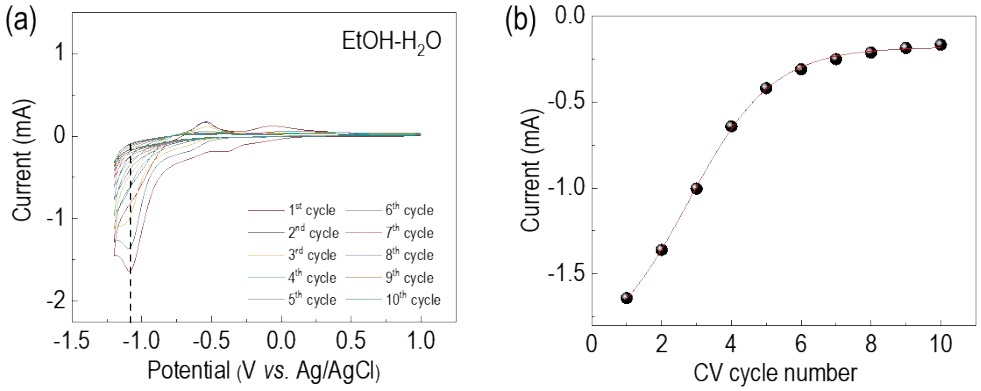

Fig. S1. (a) The 10 cycles of CV curves of P_2W_{18} based spin-coated films using 50% (wt) EtOH aqueous solution as solvent (P_2W_{18} concentration: 0.03g mL^{-1}; (b) the relationship between CV cycle number and peak current (reduction peak at the potential of -1.1 V).

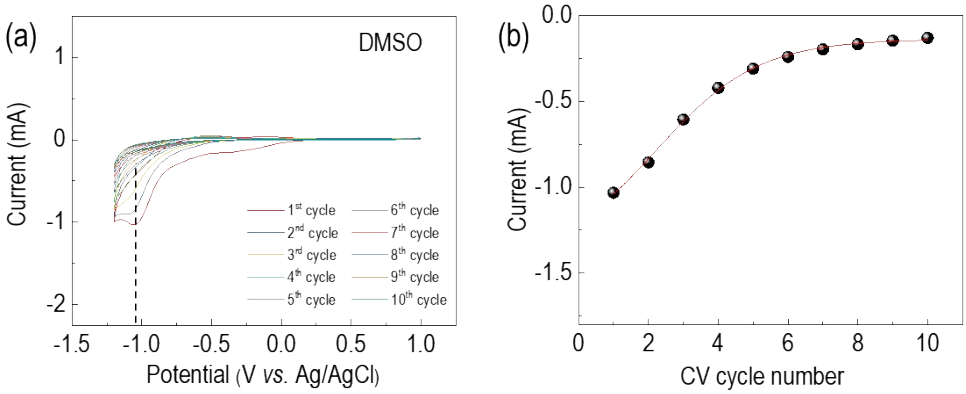

Fig. S2 (a) The 10 cycles of CV curves of P_2W_{18} based spin-coated films with DMSO as solvent (P_2W_{18} concentration: 0.03g mL^{-1}); (b) the relationship between CV cycle number and peak current (reduction peak at the potential of -1.1 V).

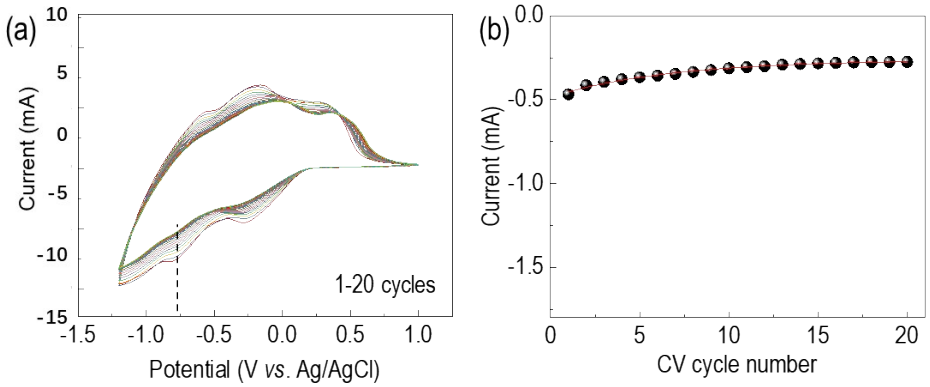

Fig. S3 (a) The 20 cycles of CV curves of P_2W_{18} based spin-coated films with PVA aqueous solution （0.3 g mL^{-1}） as solvent (P_2W_{18} concentration: 0.03g mL^{-1}); (b) the relationship between CV cycle

number and peak current (reduction peak at the potential of -0.8 V).

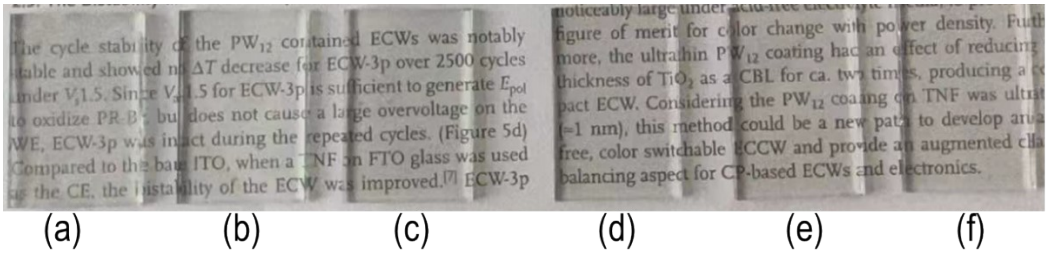

Fig. S4 the images of the as prepared P1P03 (a) , P2P03 (b), P3P02 (c), P3P03 (d), P3P04(e), P3P05 (f).

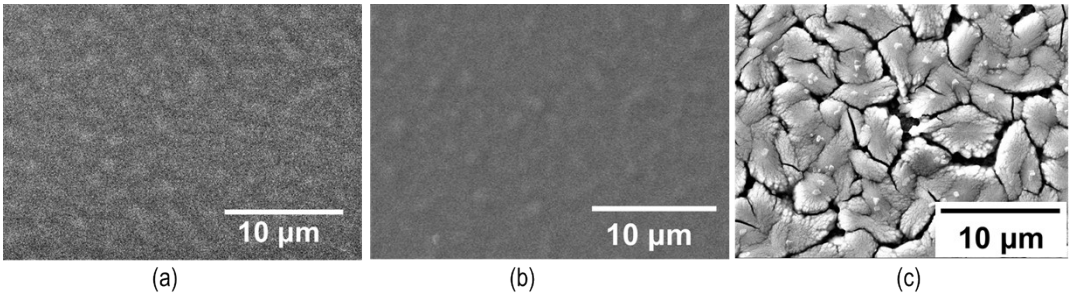

Fig. S5 (a) the top view SEM image of the P3P05 film on FTO, (b) the top view SEM image of the P3P02 film on FTO, (c) the film prepared with unreacted well P3P03

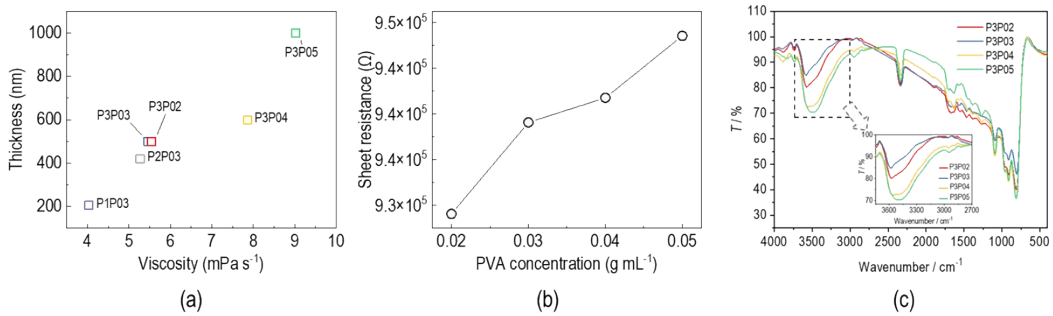

Fig. S6 (a) the relationship between the viscosity of the spin coating solution and thickness of the films. (b) the relation between the sheet resistance of the films with the PVA concentration, (c) the IR spectra of P3P02-P3P05 on Si wafer. 1 mg solution of P3P02-P3P05 was used to prepare a film on Si wafer.

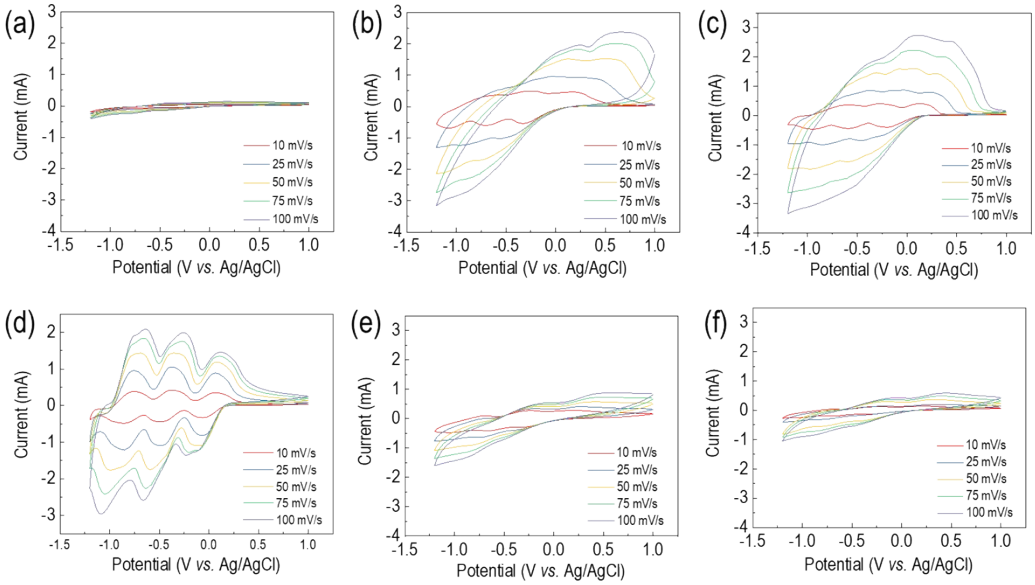

Fig. S7. Fig. S7 The CV curves of P1P03 (a), P2P03 (b), P3P02 (c), P3P03 (d), P3P04(e), P3P05 (f) under different scan rates in the 1.0M $LiClO_4$/PC solution, electrode area:2.25 cm^2.

The charge storage of the film can be obtained after calculated using **Eq. S1, S2**

$i = a\upsilon^b$ Eq. S1

$\log i = b\log \upsilon + \log a$ Eq. S2

where i and υ are peak current and scan rate, respectively; a and b are constants. If peak current (i) and scan rate (υ) have a linear relationship ($b \geq 1$), the electrode materials exhibit pseudocapacitive properties and capacitance dominated by the rapid surface Faraday reaction. Conversely, if i exhibit a square root relationship with υ (b=0.5), it suggests that the electrode materials belong to the battery type, and the charge-discharge storage process follows the typical diffusion process. When the value of b is between 0.5 and 1, the electrode materials belong to transition-type material.

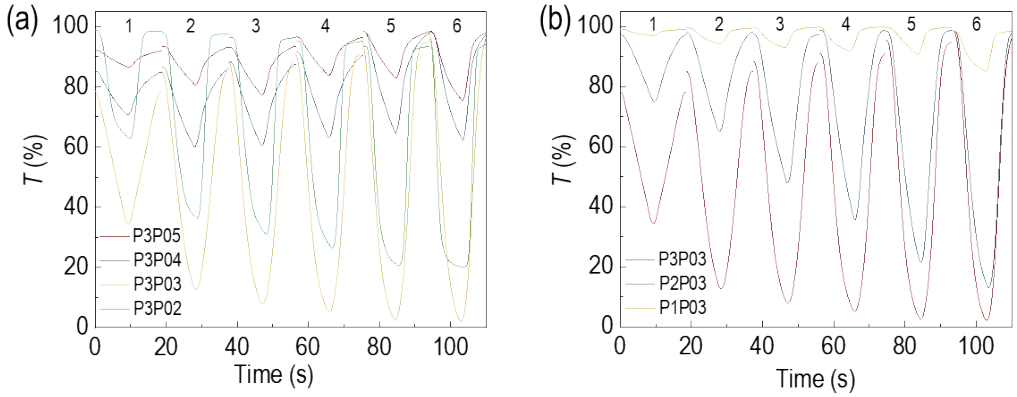

Fig S8 The transmittance changes at 580 nm under the E_{ap}s 1 (±0.4 V), 2 (±0.8 V), 3 (±1.0 V), 4 (±1.2 V), 5 (±1.5 V), 6 (±1.8 V) in 1.0 M $LiClO_4$/PC solution, each potential step last for 10 s; (a) P3P02, P3P03 , P3P04 , P3P05; (b) P1P03, P2P03, P3P03.

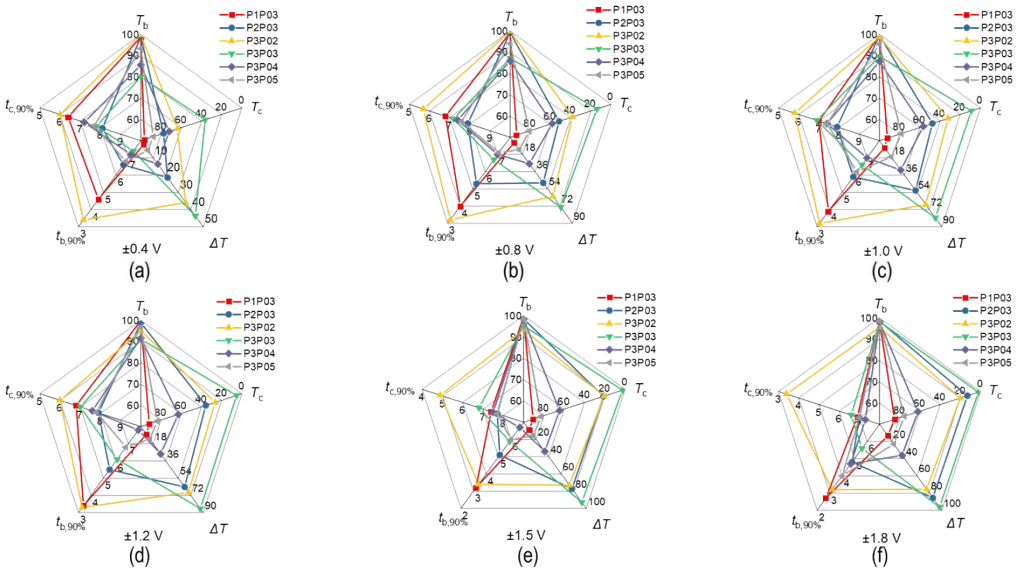

Fig. S9 the comparison of the EC performance of P1P03, P2P03, P3P02, P3P03, P3P04, P3P05 films under E_{ap} of ±0.4 (a), ±0.8 (b), ±1.0 (c), ±1.2 (d), ±1.5 (e) and ±1.8 (f) in a three-electrode system with 1.0 M $LiClO_4$/PC as electrolyte

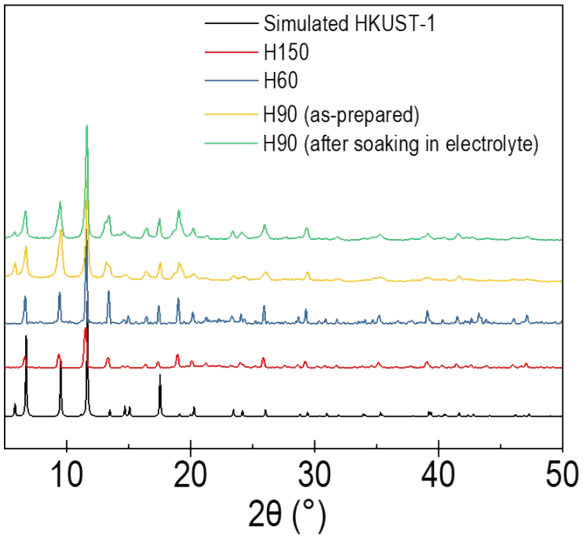

Fig. S10 the XRD pattern of H60, H90, H150 and simulated HKUST. H60, H90, H150 were scratched from the electrodeposited H60, H90, H150 film on FTO substrate. The green one represents the XRD pattern of as-prepared H90 soaking in the 1.0M $LiClO_4$/PC electrolyte for 5 days.

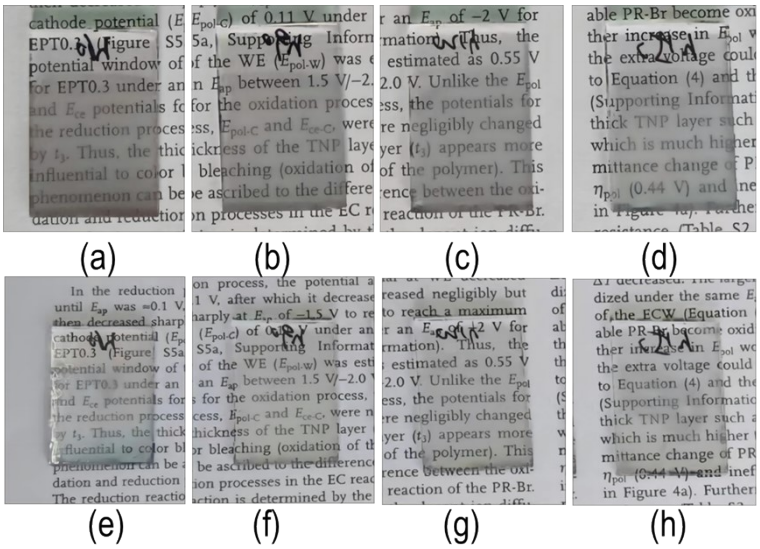

Fig. S11 the images of H60 (a), H90(b), H120(c), H150(d), H60PP(e), H90PP(f), H120PP(g), and H150PP(h).

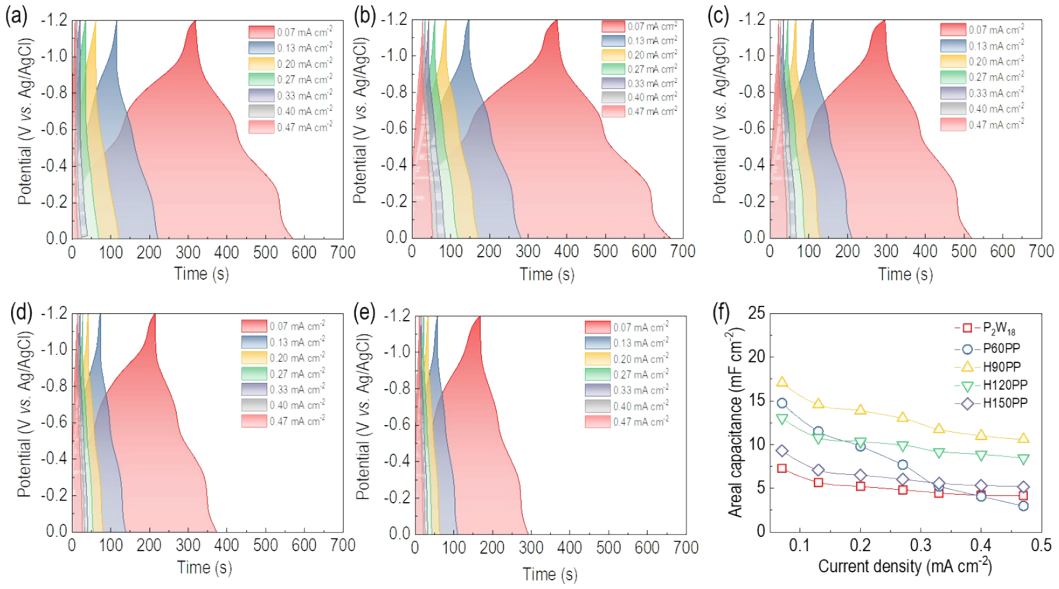

Fig. S12 the GCD curve of H60PP (a), H90PP (b), H120PP (c), H150PP (d), and PP (e) under different current density. (f) the comparison of the capacitance value under different current density

.

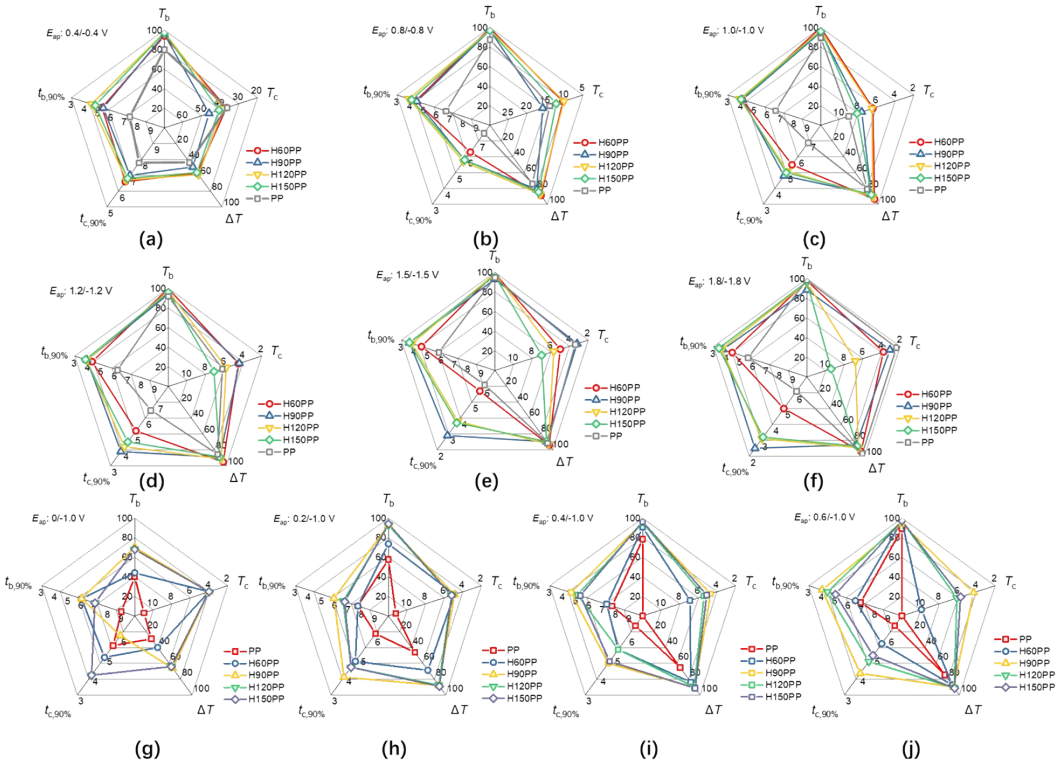

Fig S13 the EC performance comparison of the PP and HnPP (n=60,90,120,150) under the E_{ap} of ±0.4, ±0.8, ±1.0, ±1.2, ±1.5, ±1.8, 0/-1.0, 0.2/-1.0, 0.4/-1.0, 0.6/-1.0 V (a-j) in a three-electrode system with 1.0M $LiClO_4$/PC solution as electrolyte, Ag/AgCl as the reference electrode.

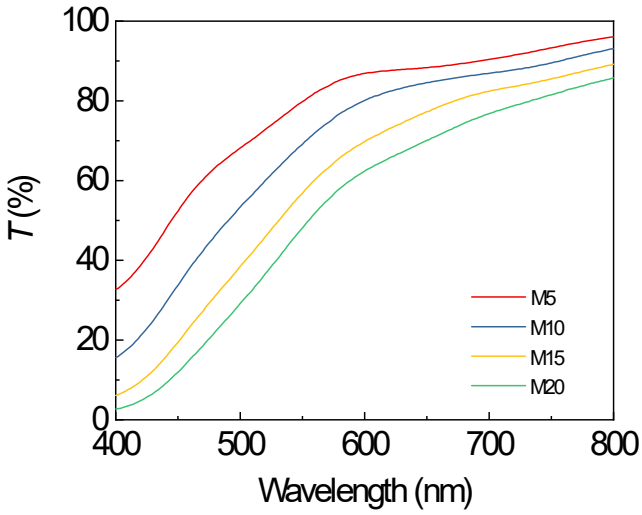

Fig. S14 the transmittance of as prepared M5, M10,M15 and M20 films, bare FTO employed as the background.

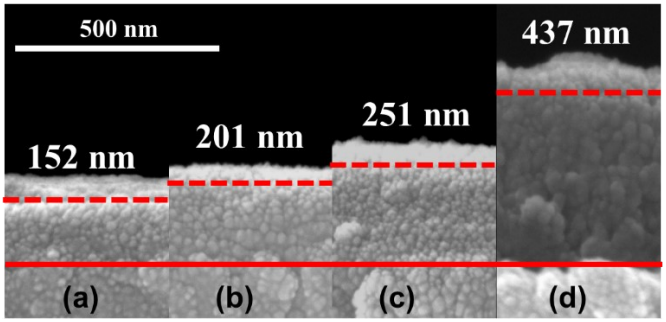

Fig. S15 the cross-section SEM of (a) 50 s, (b) 100 s, (c) 150 s, (d) 200 s electrodeposited MnO_2

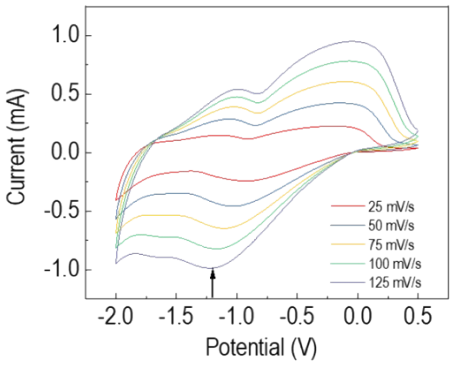

Fig. S16 the CV of H90PP//M10-EESD under different scan rates in the voltage range of -2.0 to 0.5 V.

4. Supporting tables

Table S1 The EC performance [a)] of the P1P03, P2P03, P3P02, P3P03, P3P04, P3P05 films under different E_{ap}s [b)]

Sample name	V_{ap} / V	T_b / %	T_c / %	ΔT / %	$t_{b,90\%}$ / s	$t_{c,90\%}$ / s
P1P03	±0.4	98.7	96.5	2.2	4.6	6.4
	±0.8	99.2	93.5	5.7	4	6.8
	±1	99.6	92.2	7.4	3.9	7
	±1.2	99.8	91.7	8.1	3.4	6.8
	±1.5	99.6	90.7	8.9	3.2	7.4
	±1.8	98.4	85	13.4	2.7	6.9
P2P03	±0.4	98.9	77.5	21.4	6.6	8.1
	±0.8	99.2	51.5	47.7	5.3	7.9
	±1	99.6	47.6	52	5.9	7.9
	±1.2	98.8	35.7	63.1	5.5	7.9
	±1.5	98.5	21.3	77.2	5.1	7.7
	±1.8	98.5	13	85.5	4.8	7
P3P02	±0.4	99.7	63.8	35.9	3.4	6
	±0.8	99.9	38.2	61.7	3.2	5.7
	±1	98.9	32.1	66.8	3.2	5.8
	±1.2	95.1	26.4	68.7	3.3	6
	±1.5	93.5	20.6	72.9	3.4	4.9
	±1.8	95.6	20.1	75.5	3.2	3.4
P3P03/PP	±0.4	80	36.3	43.7	7.4	7.8
	±0.8	87.1	13.9	73.2	6.7	7.2
	±1	89.6	9	80.6	6.6	6.9
	±1.2	91	5.2	85.8	6.1	7
	±1.5	95.3	2.5	92.8	5.9	6.8
	±1.8	98.3	2.1	96.2	5.6	6.6
P3P04	±0.4	85.6	72	13.6	7.2	7.2

	±0.8	85.9	58.2	27.7	7	7.4
	±1	87.3	56.6	30.7	7	7.4
	±1.2	91.6	63	28.6	7.8	7.6
	±1.5	98.4	64.6	33.8	6.7	7.5
	±1.8	98.1	62	36.1	4.7	7.3
P3P05	±0.4	93.3	87.7	5.6	6.8	7.7
	±0.8	94	81	13	7.1	7.6
	±1	95.4	78.4	17	6.2	7.4
	±1.2	96.7	83.7	13	6.8	7.8
	±1.5	98.4	82.8	15.6	6	7.7
	±1.8	98.4	75.4	23	4	7

[a)] the EC performances were measured in a three-electrode system, with Pt wire as counter electrode, Ag/AgCl as reference electrode in 1.0 M $LiClO_4$/PC solutions; b) each E_{ap} step last for 10 s

Table S2 The EC performance [a)] of the H60PP, H90PP, H120PP and H150PP films under different E_{ap}s [b)]

Sample name	V_{ap} / V	T_b / %	T_c / %	ΔT / %	$t_{b,90\%}$ / s	$t_{c,90\%}$ / s
H60PP	±0.4	94	36.6	57.4	6.6	5.3
	±0.8	99.2	10.4	88.8	6.3	4.4
	±1.0	100	6.4	93.6	5.5	4.1
	±1.2	99.6	4.5	95.1	5.2	4.3
	±1.5	99.1	5	94.1	5.7	4.5
	±1.8	97.8	3.8	94	5	4.4
	0/-1.0	44	4	40	4.9	6
	0.2/-1.0	73.6	4.9	68.7	4.7	7.7
	0.4/-1.0	90.6	6.9	83.7	5.3	7.3
	0.6/-1.0	97.3	9.9	87.4	5.6	6.5
H90PP	±0.4	95.5	46	49.5	7	5.4
	±0.8	97.1	15.8	81.3	5.8	4.5

	±1.0	95.2	7.6	87.6	4.8	4.1
	±1.2	93.8	4.4	89.4	3.9	3.9
	±1.5	93.0	3.2	89.7	2.9	3.6
	±1.8	88.5	3.1	85.4	2.5	3.7
	0/-1.0	70	4	66	6	6
	0.2/-1.0	92.8	4.9	87.9	3.9	5.9
	0.4/-1.0	95.3	4.7	90.6	4.6	4.6
	0.6/-1.0	94.2	4.3	89.9	4.1	4
H120PP	±0.4	97.4	38.2	59.2	6.7	4.5
	±0.8	97.5	10.1	87.4	5.7	3.9
	±1.0	97.1	6.5	90.6	5.1	3.9
	±1.2	97	5.8	91.2	4.2	3.9
	±1.5	98.6	5.7	92.9	3.8	3.8
	±1.8	96	6.8	89.2	3.1	3.6
	0/-1.0	68	4	64	4	7
	0.2/-1.0	92.8	5.2	87.6	4.4	6.6
	0.4/-1.0	95.3	5.4	89.9	5.3	5.1
	0.6/-1.0	97	6.1	90.9	4.7	4.4
H150PP	±0.4	97.3	40.7	56.6	6.8	4.8
	±0.8	96.8	12.2	84.6	5.8	4.1
	±1.0	96	8.1	87.9	5	4
	±1.2	95.8	7.1	88.7	4.5	3.8
	±1.5	96.5	7	89.5	3.7	3.6
	±1.8	96.8	9.4	87.4	3.2	3.4
	0/-1.0	68	4	64	4	7
	0.2/-1.0	94.1	5.2	88.9	4.4	6.7
	0.4/-1.0	96.4	5.1	91.3	4.7	5.3
	0.6/-1.0	97.2	5.7	91.5	5	5

[a)] the EC performances were measured in a three-electrode system, with Pt wire as counter electrode,

Ag/AgCl as reference electrode in 1.0 M $LiClO_4$/PC solutions; b) each E_{ap} step last for 10 s

Table S3 the comparison of the POMs EC performances between this work and the reports

No.	Name	method	electrolyte	Driving potential (voltage) / V	ΔT/%	tb	tc	cyclability	Ref.
1	TiO_2(NP)–$P_2W_{15}V_3$	Electrodeposition	0.1 M HCl aqueous solution	3.1	91.8	3.5	3.9	1000	[5]
2	TiO_2(NP)–$P_2W_{16}V_2$	Electrodeposition	0.1 M HCl aqueous solution	2.9	48.3	11.1	4.5	1000	
3	TiO_2(NP)–$P_2W_{17}V$	Electrodeposition	0.1 M HCl aqueous solution	3.2	85.1	5.6	4.1	1000	
4	TiO_2(NP)–W_{10}	Electrodeposition	0.1 M H_2SO_4 aqueous solution	1.3	49.5	7.2	4.9	100	[6]
5	$[P_2W_{18}$/PAH/P_2W_{18}/ $TiO_2]_{10}$	LBL	pH 2.0 HCl solution	1.4	24	15.4	13.4	1000	[7]
6	(PDDA/W_{10})n (n = 3)	LBL	0.1 M aqueous NaCl at pH = 2.5	1.2	5.6	5	65	58	[8]
7	(PSS/PAH/Eu-P_5W_{30}/PAH)$_{20}$	LBL	pH 3.0 buffer solutions	1.2	19			500	[9]
8	$[P_2W_{18}$/PAH/P_2W_{18}/ $TiO_2]_{10}$	LBL	pH 2.0 HCl solution	2.5	24	15.4	13.4	50	[7]
9	PSS/Cu(phen)$_2$/$[(P_2W_{17}$/Cu(phen)$_2)]_{30}$	LBL	0.2 M HOAc–NaOAc buffer at pH = 3.5	1.4	43	6.6	6.5	200	[10]
10	PSS/Fe(phen)$_3$/$[(P_2W_{17}$/Fe(phen)$_3)]_{30}$	LBL	0.2 M HOAc–NaOAc buffer at pH = 3.6	1.4	40	7.4	7	200	[10]
11	PEI/$[SiW_9V_3$/PEI–$Bi_2O_3]_{15}$/ SiW_9V_3	LBL	0.2 M HOAc–NaOAc (pH = 3.82) buffer solutions.	1.0	6.7	7	6.3	10	[11]
12	{[Ce(P_2W_{17})$_2$]/PAH}$_{20}$	LBL	0.1 M HOAc–NaOAc buffer solution (pH B 4.0)	0.9	34	4	5.5	200	[12]
13	PSS/PAH/(P_2W_{15}/PAH)$_{20}$	LBL	HOAc–NaOAc buffer solution (pH 4.0)	0.8	44	5.5	6	300	[13]
14	$[P_2W_{18}$/CS-CNTs]$_{30}$	LBL	HOAc–NaOAc buffer solution (pH = 4)	1.4	20.3	4.3	3.7	200	[14]
15	PSS(PEI/PSS)$_3$(PEI/$W_{18}O_{49}$)$_{30}$/ (PEI/P_8W_{48})$_{20}$	LBL	0.10 M $LiClO_4$ aqueous solution	1.4	35	26	86	500	[15]

			(pH = 5.0)						
16	Nano-SnO_2/PDDA/[$PMo_{12}O_{40}$]	LBL	0.1M Na_2SO_4 (PH=5.5)	0.9	11	1	1	25	[16]
17	TiO_2(NP)–Na-P_5W_{30}	Electrodeposition	0.1 M LiI /PC	2.0	50	1	1	1000	[17]
18	TiO_2(NP)–$PW_{11}V$	Electrodeposition	0.1 M $LiClO_4$ PC solution	3.8	44	15.6	8.7	1000	
19	TiO_2(NP)–$PW_{10}V_2$	Electrodeposition	0.1 M $LiClO_4$ PC solution	3.8	66	17.2	6.4	1000	[18]
20	TiO_2(NP)–PW_9V_3	Electrodeposition	0.1 M $LiClO_4$ PC solution	3.8	77	7.1	2.4	1000	
21	{PEI/[$P_2W_{17}V$/PEI-CdS]$_{30}$}$P_2W_{17}V$	LBL	0.05 M NaH_2PO_4–Na_2HPO_4 buffer solutions (pH = 7.0)	1.1	59.8	5.6	2.4	100	[19]
22	[PEI/P_2W_{18}/PEI/WO_3]$_{20}$	LBL	1 M $LiClO_4$ PC solution	3.0	48.4	24.9	2.4	500	[20]
23	H90PP	spin coating		3	90	2.9	3.6	1650	this work
24	PP	spin coating						750	this work

Reference

[5] L. Liu, S.-M. Wang, C. Li, C.-G. Liu, C.-L. Ma, Z.-B. Han, Pure inorganic multi-color electrochromic thin films: vanadium-substituted Dawson type polyoxometalate based electrochromic thin films with tunable colors from transparent to blue and purple, J. Mater. Chem. C 3(20) (2015) 5175-5182. https://doi.org/10.1039/C4TC02947J.

[6] Z. Kim, Q.-C. Guo, S.-M. Wang, Q. Wu, Z.-B. Han, The preparation of decatungstate based high performance electrochromic film, Thin. Solid. Films. 639 (2017) 1-6. https://doi.org/10.1016/j.tsf.2017.08.018.

[7] S. Liu, L. Xu, G. Gao, B. Xu, W. Guo, Electrochromic multilayer films with enhanced stability based on polyoxometalate and TiO2, Mater. Chem. Phys. 116(1) (2009) 88-93. https://doi.org/10.1016/j.matchemphys.2009.02.054.

[8] I. Moriguchi, J.H. Fendler, Characterization and Electrochromic Properties of Ultrathin Films Self-Assembled from Poly(diallyldimethylammonium) Chloride and Sodium Decatungstate, Chem. Mater. 10(8) (1998) 2205-2211. https://doi.org/10.1021/cm980127b.

[9] S. Liu, D.G. Kurth, H. Möhwald, D. Volkmer, A Thin-Film Electrochromic Device Based on a Polyoxometalate Cluster, Adv. Mater. 14(3) (2002) 225-228. https://doi.org/10.1002/1521-4095(20020205)14:3<225::AID-ADMA225>3.0.CO;2-F.

[10] G. Gao, L. Xu, W. Wang, W. An, Y. Qiu, Z. Wang, E. Wang, Electrochromic Multilayer Films of Tunable Color by Combination of Copper or Iron Complex and Monolacunary Dawson-Type Polyoxometalate, J. Phys. Chem. B 109(18) (2005) 8948-8953. https://doi.org/10.1021/jp044403n.

[11] C. Li, K.P. O'Halloran, H. Ma, S. Shi, Multifunctional Multilayer Films Containing Polyoxometalates and Bismuth Oxide Nanoparticles, J. Phys. Chem. B 113(23) (2009) 8043-8048. https://doi.org/10.1021/jp9001498.

[12] G. Gao, L. Xu, W. Wang, W. An, Y. Qiu, Electrochromic ultra-thin films based on cerium polyoxometalate, J. Mater. Chem. 14(13) (2004) 2024-2029. https://doi.org/10.1039/B400021H.

[13] G. Gao, L. Xu, W. Wang, Z. Wang, Y. Qiu, E. Wang, Electrochromic multilayer films based on trilacunary Dawson-type polyoxometalate, Electrochim. Acta. 50(5) (2005) 1101-1106. https://doi.org/10.1016/j.electacta.2004.08.006.

[14] S. Liu, L. Xu, F. Li, W. Guo, Y. Xing, Z. Sun, Carbon nanotubes-assisted polyoxometalate nanocomposite film with enhanced electrochromic performance, Electrochim. Acta. 56(24) (2011) 8156-8162. https://doi.org/10.1016/j.electacta.2011.05.131.

[15] H. Gu, C. Guo, S. Zhang, L. Bi, T. Li, T. Sun, S. Liu, Highly Efficient, Near-Infrared and Visible Light Modulated Electrochromic Devices Based on Polyoxometalates and W18O49 Nanowires, ACS. Nano. 12(1) (2018) 559-567. https://doi.org/10.1021/acsnano.7b07360.

[16] S. Usai, J.J. Walsh, Facile assembly of polyoxometalate-polyelectrolyte films on nano-MO2 (M = Sn, Ti) for optical applications, J. Electroanal. Chem. 815 (2018) 86-89. https://doi.org/10.1016/j.jelechem.2018.03.007.

[17] S.-M. Wang, L. Liu, W.-L. Chen, Z.-M. Zhang, Z.-M. Su, E.-B. Wang, A new electrodeposition approach for preparing polyoxometalates-based electrochromic smart windows, J. Mater. Chem. A 1(2) (2013) 216-220. https://doi.org/10.1039/C2TA00486K.

[18] S.-M. Wang, L. Liu, Z.-Y. Huang, Z.-B. Han, Vanadium substituted Keggin-type POM-based electrochromic films showing high performance in a Li+-based neutral non-aqueous electrolyte, RSC. Adv. 6(45) (2016) 38782-38789. https://doi.org/10.1039/C6RA03037H.

[19] D. Zhang, Y. Chen, H. Pang, Y. Yu, H. Ma, Enhanced electrochromic performance of a vanadium-

substituted tungstophosphate based on composite film by incorporation of cadmium sulfide nanoparticles, Electrochim. Acta. 105 (2013) 560-568. https://doi.org/10.1016/j.electacta.2013.05.042.
[20] S. Liu, Layer-by-layer assembled WO3 and tungstophosphate nanocomposite with enhanced electrochromic properties, J. Mater. Sci.: Mater. Electron. 27(10) (2016) 11118-11125. https://doi.org/10.1007/s10854-016-5229-3.